

Canopy Carbon Gain and Water Use: Analysis of Old-growth Conifers in the Pacific Northwest

William E. Winner,^{1*} Sean C. Thomas,² Joseph A. Berry,³ Barbara J. Bond,⁴
Clifton E. Cooper,¹ Thomas M. Hinckley,⁵ James R. Ehleringer,⁶
Julianna E. Fessenden,⁶ Brian Lamb,⁷ Sarah McCarthy,⁵
Nate G. McDowell,⁴ Nathan Phillips,⁴ and Mathew Williams⁸

¹Department of Botany and Plant Pathology, Oregon State University, Corvallis, Oregon 97331, USA; ²Faculty of Forestry, University of Toronto, Toronto, Canada; ³Department of Plant Biology, Carnegie Institute of Plant Biology, Stanford, California 94305, USA; ⁴Forest Science Department, Oregon State University, Corvallis, Oregon 97331, USA; ⁵College of Forest Resources, University of Washington, Seattle, Washington 98915, USA; ⁶Biology Department, University of Utah, Salt Lake City, Utah 84112, USA; ⁷Department of Civil and Environmental Engineering, Washington State University, Pullman, Washington 99164, USA; ⁸The Ecosystems Center, Marine Biological Laboratory, Woods Hole, Massachusetts 02543, USA

ABSTRACT

This report summarizes our current knowledge of leaf-level physiological processes that regulate carbon gain and water loss of the dominant tree species in an old-growth forest at the Wind River Canopy Crane Research Facility. Analysis includes measurements of photosynthesis, respiration, stomatal conductance, water potential, stable carbon isotope values, and biogenic hydrocarbon emissions from Douglas-fir (*Pseudotsuga menziesii*), western hemlock (*Tsuga heterophylla*), and western red cedar (*Thuja plicata*). Leaf-level information is used to scale fluxes up to the canopy to estimate gross primary production using a physiology-based process model. Both light-saturated and in situ photosynthesis exhibit pronounced vertical gradients through the canopy, but are consistently highest in Douglas-fir, intermediate in western hemlock, and lowest in western red cedar. Net photosynthesis and stomatal conductance are strongly dependent on vapor-pressure deficit in Douglas-fir, and decline through the course of a

seasonal drought. Foliar respiration is similar for Douglas-fir and western hemlock, and lowest for western red cedar. Water-use efficiency varied with species and tree height, as indexed using stable carbon isotope values for foliage. Leaf water potential is most negative for Douglas-fir and similar for western hemlock and western red cedar. Terpene fluxes from foliage equal approximately 1% of the net carbon loss from the forest. Modeled estimates based on physiological measurements show gross primary productivity (GPP) to be about 22 Mg C m⁻² y⁻¹. Physiological studies will be necessary to further refine estimates of stand-level carbon balance and to make long-term predictions of changes in carbon balance due to changes in forest structure, species composition, and climate.

Key words: biogenic carbon emissions; canopy processes; forest carbon budget; forest gas exchange; old-growth canopy.

Received 15 February 2002; accepted 28 March 2003; published online 19 May 2004.

*Corresponding author; e-mail: winnerw@bcc.orst.edu

INTRODUCTION

The impetus to understand and predict the storage of carbon in forest ecosystems worldwide has grown dramatically over the last decade in response

to the global challenge of increasing atmospheric carbon dioxide (CO_2). One approach for predicting ecosystem-scale storage and fluxes of carbon is to make measurements at scales below the ecosystem to understand the mechanisms that control carbon flux. Measurements of leaf- and canopy-level carbon assimilation over the daily, season, and annual time scales provide information that can be used to understand the linkages between environmental factors and physiological processes, which can then be scaled to estimate ecosystem fluxes. However, measurements of physiological processes have rarely been made for large, old trees (Ryan and others 1997). Because leaf-level carbon and water fluxes can vary with tree size and age (Gower and others 1996; Ryan and others 1997; Thomas and Winner 2002), and are closely linked to ecosystem carbon fluxes that also vary with stand development (Schulze and others 2000), there is a need for studies examining leaf-level physiology in relation to ecosystem-scale carbon cycling in old forests.

Physiological studies have focused on young rather than old trees in large part because of the difficulty of accessing canopies of old trees. The Wind River canopy crane provides an opportunity for such studies in a coniferous forest that is exceptional both in terms of tree size (up to 65 m high) and age (dominant trees are 450–500 years old). Numerous studies of foliage and the canopy as a whole are under way. Research includes analysis of diurnal and seasonal analyses of net photosynthesis (A), stomatal conductance (g_s), respiration (R), and water potential (Ψ_1) (Bauerle and others 1999; Cooper and others in press; McDowell and others 2002; Thomas and Winner 2002), measurements of biogenic hydrocarbon fluxes (Pressley and others in review), and determination of $\delta^{13}\text{C}$ for leaves and ecosystem components (Fessenden and Ehleringer 2002; McDowell and others 2002). Simultaneous with these analyses of foliage and canopies are measurements of ecosystem-scale carbon flux and storage (Chen and others 2002; Harmon and others 2004; Paw U and others 2004), water fluxes (Phillips and others 2002; Unsworth and others 2004), and canopy structure (Thomas and Winner 2000; Parker and others 2004). The integration of work at both the leaf scale and the ecosystem scale provides an opportunity to examine the mechanisms that regulate carbon and water fluxes from this forest. Here we use a physiologically based process model (Williams and others 1996) to apply our information on leaf-level use of carbon and water to derive independent predictions of annual gross primary productivity (GPP). Process model-based estimates of GPP can then be

compared to those based on eddy covariance (Paw U and others 2004) and inventory-based assessments (Harmon and others 2004).

Gas-exchange measurements can help account for net photosynthetic carbon gain, which is the difference between total carbon assimilated minus carbon lost by respiration. However, plants also lose carbon by emissions of biogenic hydrocarbon (BHC) molecules (Sharkey and others 1991a, 1991b). BHCs, such as isoprene and the monoterpenes, are emitted from many plant species and, at least in some forests, may equal the net uptake of CO_2 annually (Guenther and others 1995). BHCs emitted from living vegetation are highly reactive in the atmosphere and contribute to the photochemical processes that produce ozone (Fehsenfeld and others 1992), organic acids, organic nitrates, carbon monoxide, and aerosols (Jacob and Wofsy 1988; Rasmussen and Khalil 1988; Talbot and others 1988).

Our first objective is to compare and summarize leaf-level physiology of the dominant tree species in the old forest surrounding the Wind River canopy crane. We focus our analysis on the controls over carbon assimilation, stomatal conductance, and water-use efficiency because these parameters play a critical role in regulating carbon assimilation at the canopy scale. We also address the controls over hydrocarbon emissions and investigate the possibility that these emissions are a significant component of the ecosystem carbon budget. Our second objective is to use our results in an empirically parameterized soil–plant–atmosphere model [SPA (Williams and others 1996)] to predict GPP fluxes for 1999. Special attention is paid to putting analysis of carbon flux determined from physiologically based measurements into context with estimates of carbon flux made by scientists using independent methods at the site.

The SPA model used here to predict whole-forest carbon flux makes a number of assumptions regarding forest canopy physiology that represent hypotheses about how the ecosystem “works.” A central model assumption is that carbon gain per unit leaf nitrogen (N) is maximized for each canopy layer, under the constraint that stomatal conductance adjusts so that transpiration is balanced by water supply (Williams and others 1996). We expect that hydraulic path-length effects on water transport should result in an especially pronounced role of hydraulic limitation on gas-exchange processes in very tall forests (Ryan and others 1997; Hubbard and others 1999). The forest at Wind River is dominated by a mix of the long-lived, early successional Douglas-fir (*Pseudotsuga menziesii*) and

the late successional species western hemlock (*Tsuga heterophylla*) and western red cedar (*Thuja plicata*). Although the SPA model assumes that all canopy leaves at a given vertical position behave similarly, we expect that species may show strong physiological differences related to successional status. Finally, because the net carbon balance in any old-growth ecosystem is likely closer to zero than in regenerating ecosystems, we hypothesized that volatile organic hydrocarbons would be a relatively large component of net carbon exchange in the old-growth forest ecosystem at Wind River.

METHODS

Gas-exchange Measurements

Measurements of A and g_s were made using a Li-Cor 6400 portable photosynthesis system (Li-Cor, Lincoln, NE, USA). Seasonal surveys (conducted in March, June, September, and December of each year) of A and g_s were made on the youngest, fully expanded needle cohort. The seasonal surveys commenced in September 1996. Measurements included both in situ gas exchange, with photosynthetically active radiation (PAR) levels matched to ambient conditions (using a Li-190 quantum sensor), and photosynthetic capacity measured under saturating PAR levels of 1200–1500 $\mu\text{mol quanta m}^{-2} \text{ s}^{-1}$, in that order. Gas-exchange measurements were performed upon 2–3 trees per species, with three branchlets measured per sampling period for each tree, at both upper-canopy and lower-canopy positions.

Photosynthetic capacity measurements were made prior to midday or late-day stomatal closure. PAR levels were manipulated using a Li-6400-02 red light-emitting diode light source. After a change in the PAR level, foliage was allowed to achieve full light induction prior to recording measurements. Relationships between photosynthesis and internal CO_2 (termed A/c_i curves) were also measured with a Li-Cor 6400 with the light source set to PAR values of 1400 $\mu\text{mol quanta m}^{-2} \text{ ground area s}^{-1}$. Dark-acclimated foliar respiration measurements at ambient temperature were made on a subset of samples, using a Li-Cor 6400, subsequent to photosynthesis measurements. Respiration measurements commenced in September 1997. Temperature coefficient (Q_{10}) values were estimated using nonlinear regression of respiration (R) on leaf temperature, using the function $R = x e^{zT}$ (where x and z are fitted constants) with Q_{10} calculated as e^{10z} .

Water-potential Measurements

Bulk tissue water potential (Ψ_1) was measured concurrent with gas-exchange measurements using Scholander-type pressure chambers (PMS, Corvallis, OR, USA). Samples for water-potential measurements were collected from branches 1 m or less in distance from the branches used for gas-exchange studies and were assumed to be physiologically similar to those measured for photosynthesis and respiration rates. Measurements were made on twigs approximately 3 mm in diameter sampled from at least three clipped branches at each location in the canopy. Samples were stored in plastic bags until analysis within 30 min of collection.

Stable-isotope Analysis

Stable carbon isotopes of plant material ($\delta^{13}\text{C}_p$) provide an assimilation-weighted, or time-integrated, measure of both g_s and A , and are therefore a powerful tool to determine water-use efficiency (WUE) during the period of leaf growth and for comparison of WUE between species. When c_i (intercellular CO_2 concentration) is low, WUE is high, and the leaf assimilates more $^{13}\text{CO}_2$ relative to $^{12}\text{CO}_2$ than when c_i is high. In addition, $\delta^{13}\text{C}_p$ analyses may be used to estimate long-term ratios of the intercellular to ambient CO_2 values (c_i/c_a) if the carbon isotope ratio of atmospheric CO_2 ($\delta^{13}\text{C}_a$) is known (Farquhar and others 1989; Ehleringer and others 1993). To learn about c_i and WUE values for foliage of trees at the Wind River site, foliar samples were collected from the three dominant tree species within the stand—Douglas-fir, western hemlock, and western red cedar—and from the representative understory species: Pacific silver fir (*Abies amabilis*), vine maple (*Acer circinatum*), Oregon grape (*Berberis nervosa*), and feather moss (*Plagiothesium undulatum*). Foliar samples were collected from three separate trees, herbaceous plants, and moss patches for each species type. For understory measurements, about 0.5 g of current-year leaves were sampled from Oregon grape and feather moss growing in shaded regions. For canopy measurements, about 0.5 g of current-year needles were collected from south-facing branches located at 53 m and at 24 m for each of the nine trees sampled. Each branch was resampled once per month from March 1999 to October 1999. Data presented originated from foliar samples and canopy CO_2 samples taken in May 1999. Foliar samples taken in September 1999 were matched to in situ gas-exchange measurements. All foliar materials

were oven dried on site for 48 h and then ground with mortar and pestle and analyzed on a Finnigan Delta S mass spectrometer (Isotech Laboratories, Champaign, IL, USA) located within the laboratory. The precision was $\pm 0.02\text{‰}$ for $\delta^{13}\text{C}$ in ambient CO_2 , and $\pm 0.05\text{‰}$ for $\delta^{13}\text{C}$ in foliar samples.

Biogenic Hydrocarbon Emissions

Emissions of BHCs were measured for Douglas-fir, western hemlock, western red cedar, and Pacific silver fir. Measurements were restricted to monoterpenes collected using a 4-L branch chamber designed for the purpose. At the onset of the sampling program, monoterpene emission samples were collected from each tree species to identify the major and minor components of the hydrocarbon emissions. Sampled branches were healthy and representative, and included shoot apices and foliated internodes representing the most recent 2–3 years of growth. First-year foliage represented approximately 50% of enclosed biomass. A total of 106 emission samples were collected from eight Douglas-fir branches (one tree), and 89 samples from eight western hemlock branches (one tree) over both measurement seasons. Sampling was restricted to one tree of each species to preserve the long-term integrity of the site. Our samples were thus pseudo-replicated, and although the trees were chosen to be as representative of the stand as possible, biases may result if the available amounts of water or nutrients were unusually high or low. Samples for qualitative analysis were collected on site and returned to Washington State University for analyses using gas chromatography–mass spectrometry. Monoterpene emissions were quantified using gas chromatography–flame ionization detection (Westberg and Zimmerman 1993) during the summer of 1997. Details of these measurements are provided by Pressley and colleagues (in press).

Seasonal changes in BHC emissions may be the result of temperature change and changes in physiological processes (Croteau 1987). Monoterpenes are produced and stored in resin ducts along the subsurface of the needle. The emission rate is controlled by the vapor pressure of the terpene pool and by characteristics of the diffusion pathway in the needle. We modeled terpene emissions as an exponential function of leaf temperature, following prior studies [for example, see Guenther and others (1993)]. Emissions of BHCs can increase if needles are broken by mechanical stress (Juuti and others 1990) or injured by herbivory. However, such increases are thought to be temporary (Litvak 1997) and were not evaluated in this study.

Modeling

The SPA canopy model is a multilayer simulator of C_3 vascular plant processes and uses physiological measurements to simulate productivity in a variety of ecosystems (Williams and others 1996, 1998; Law and others 2000). The SPA model was applied to the forest at the Wind River site using 10 canopy layers and a 30-min time step (Williams and others 1998). The canopy structure is described by vertical variations among canopy layers in light-absorbing area [light-area index (LAI)], photosynthetic capacity (related to foliar N), and plant hydraulic properties. The model has a detailed radiation-transfer scheme that calculates sunlit and shaded fractions of the foliage in each canopy layer. The maximum rate of carboxylation (V_{cmax}) and the maximum rate of electron transport (J_{max}) are determined from A/c_i curves derived from leaf-level gas-exchange studies as already described. The model adjusts g_s to balance atmospheric demand for water with rates of water uptake and supply from soils. Stomatal conductance is varied to maintain transpiration (E) at the level that keeps Ψ_1 from falling below a critical threshold value ($\Psi_{1\text{min}}$), below which cavitation of the hydraulic system may occur. Simulation of water uptake by roots from soils requires input describing the gravitational component of leaf water potential, the plant hydraulic resistance of each canopy layer, the belowground resistance to water uptake, the distribution of roots below ground, and the soil water conductance.

The simulations for the Wind River site assume a 60-m-tall canopy with foliage distributed from 15 to 60 m, with the 10 individual layers arranged at 5-m intervals. Total canopy LAI was set to $9.6 \text{ m}^2 \text{ m}^{-2}$ and assumed to be constant throughout the year; 10% percent of canopy LAI was allocated to each layer. We parameterized a biochemical model of photosynthesis (Farquhar and von Caemmerer 1982) using in situ measurements of A/c_i curves derived from sunlit foliage in the upper canopy of Douglas-fir to estimate the maximum velocity of ribulose biphosphate (RuBP) carboxylation (V_{cmax}) and light-saturated potential rate of electron transport (J_{max}) for the upper-canopy layer. The SPA model estimates V_{cmax} and J_{max} for more shaded canopy layers by assuming an exponential decrease through the canopy (falling in the bottommost canopy layer to 40% of values in the topmost layer), corresponding to the gradient in leaf N content. Soil moisture retention curves and the relationships between soil hydraulic conductivity and soil moisture were estimated from soil

Table 1. Photosynthesis, Respiration, and Leaf Water-potential Values

	Photosynthesis		Respiration ($\mu\text{mol C m}^{-2} \text{ s}^{-1}$)	Water Potential (MPa)
	High Light ($\mu\text{mol C m}^{-2} \text{ s}^{-1}$)	In situ ($\mu\text{mol C m}^{-2} \text{ s}^{-1}$)		
Douglas-fir				
March	8.4 \pm 1.9 (6)	3.5 \pm 1.8 (6)	-2.0 \pm 0.4 (6)	-2.2 \pm 0.2 (7)
June	12.7 \pm 0.7 (11)	9.0 \pm 0.8 (11)	-1.4 \pm 0.3 (7)	-2.0 \pm 0.1 (4)
September	13.3 \pm 1.0 (6)	13.3 \pm 1.0 (6)	-1.3 \pm 0.2 (6)	-2.4 \pm 0.2 (6)
December	8.1 \pm 1.1 (6)	2.8 \pm 0.6 (6)	-0.5 \pm 0.1 (6)	-0.5 \pm 0.1 (8)
Western hemlock				
March	5.5 \pm 0.5 (9)	4.9 \pm 0.7 (9)	-2.0 \pm 0.2 (9)	-1.6 \pm 0.3 (8)
June	5.8 \pm 0.9 (6)	4.7 \pm 1.2 (6)	-3.3 \pm 0.5 (6)	-1.4 \pm 0.1 (4)
September	8.3 \pm 0.6 (9)	8.3 \pm 0.6 (9)	-1.2 \pm 0.2 (9)	-1.4 \pm 0.2 (9)
December	7.7 \pm 0.6 (6)	2.4 \pm 0.3 (6)	-0.6 \pm 0.1 (6)	-0.3 \pm 0.0 (7)
Western red cedar				
March	1.4 \pm 0.3 (6)	1.0 \pm 0.3 (6)	-0.5 \pm 0.1 (6)	-0.9 \pm 0.0 (4)
June	5.1 \pm 0.5 (6)	5.1 \pm 0.5 (6)	-1.0 \pm 0.1 (6)	-1.7 \pm 0.1 (4)
September	4.4 \pm 0.4 (6)	4.3 \pm 0.4 (6)	-1.0 \pm 0.2 (6)	-1.2 \pm 0.2 (6)
December	4.5 \pm 0.8 (6)	1.9 \pm 0.4 (6)	-0.3 \pm 0.1 (5)	-0.4 \pm 0.0 (6)

Photosynthesis, respiration, and leaf-water potential values [mean \pm SE (n)] for tops of ecologically dominant trees sampled at the Wind River canopy crane site in 1999. All photosynthesis and respiration values are expressed on the basis of carbon flux per unit silhouette area of intact, articulated foliage. "High" light intensities used were 1500 $\mu\text{mol quanta m}^{-2} \text{ s}^{-1}$ in March, June, and September, and 1200 $\mu\text{mol quanta m}^{-2} \text{ s}^{-1}$ in December.

texture (Saxton and others 1986). Rooting depth was assumed to be 1.5 m, with roots distributed in the 15 soil layers, each 0.1 m thick. Total root length was set to 3000 m m^{-2} , with root biomass declining exponentially with depth in the soil profile. Root resistivity was set to equal 400 MPa s g mmol^{-1} , and plant hydraulic conductivity was set to 20 $\text{mmol}^{-1} \text{ m}^{-1} \text{ s}^{-1} \text{ MPa}^{-1}$.

RESULTS

Carbon Use and Water Use in Canopies

Canopy Position and Light. Photosynthesis varied seasonally for the three dominant species (Table 1). Under conditions of ambient light and CO_2 , Douglas-fir typically had the highest A , followed by western hemlock and western red cedar. For all three species, in situ photosynthesis was higher in June and September in comparison to March and December. Ambient light levels typically limited photosynthesis. Douglas-fir A increased under artificial conditions of high light availability in all seasons ($\text{PAR} = \sim 1000 \mu\text{mol m}^{-2} \text{ s}^{-1}$) except for September. Western hemlock and western red cedar had increased photosynthesis in response to increases in light, but light responses were marginal during the summer. All species, however, exhibited at least a twofold increase in A with saturating-light availability in the winter months.

Photosynthetic light-response curves differed significantly among species when the relationship between A and ambient PAR are pooled across canopy heights and season (Figure 1). The slope of A/PAR (the realized quantum use efficiency) was similar for the three species: $0.093 \pm 0.004 \text{ mol C mol}^{-1} \text{ quanta}$ for Douglas-fir, $0.098 \pm 0.006 \text{ mol C mol}^{-1} \text{ quanta}$ for western hemlock, and $0.094 \pm 0.011 \text{ mol C mol}^{-1} \text{ quanta}$ for western red cedar. The plateau of the light-response curves (photosynthetic capacity) was approximately 9 $\mu\text{mol m}^{-2} \text{ s}^{-1}$ for Douglas-fir versus approximately 5 in western hemlock and approximately 4 in western red cedar. A saturated at PAR values near approximately 950 $\mu\text{mol quanta m}^{-2} \text{ s}^{-1}$ for Douglas-fir, approximately 550 $\mu\text{mol quanta m}^{-2} \text{ s}^{-1}$ for western hemlock, and 400 $\mu\text{mol quanta m}^{-2} \text{ s}^{-1}$ for western red cedar. The high variability in A at a given light level shown is attributable to seasonal and diurnal variation, tree-to-tree variation, and environmental factors other than light, such as water stress, that may limit carbon gain even when light is high.

Douglas-fir is an ecologically important and abundant species in the Pacific Northwest, accounting for 28% of the leaf area of the forest at the Wind River canopy crane (Thomas and Winner 2000). Douglas-fir displayed the highest photosynthetic rates of the three dominant conifers, particularly in high light (Table 1 and Figure 1).

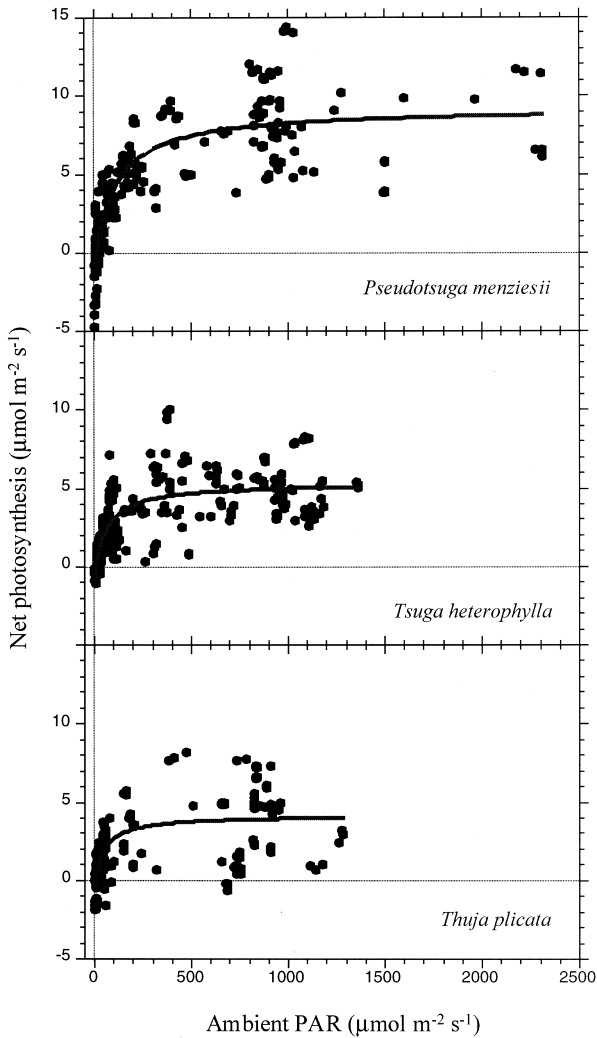


Figure 1. Photosynthetic carbon uptake for dominant tree species at the Wind River canopy crane site, expressed on a displayed leaf-area basis, as a function of ambient light levels. Data are for measurements made through the annual cycle in 1996–97 under ambient light conditions, pooling the lower, middle, and upper portions of the crown for each species. PAR, photosynthetically active radiation.

The crowns of Douglas-fir were also in the highest light environment of all species in the forests, with a midcrown average height of 35 m (Parker and others 2004). Therefore, Douglas-fir is likely to exert significant control over carbon uptake of this forest. On the basis of A/c_i curves, upper-canopy foliage for Douglas-fir showed a maximum velocity of RuBP carboxylation (V_{cmax}) of $39 \mu\text{mol m}^{-2} \text{s}^{-1}$ and a light-saturated potential rate of electron transport (J_{max}) of $129 \mu\text{mol m}^{-2} \text{s}^{-1}$.

Respiration. Foliar respiration rates measured at ambient temperatures were similar for Douglas-fir

and western hemlock, except in June, when respiration in hemlock was higher. Respiration in western red cedar was generally lower (Table 1). Q_{10} values were computed using in situ foliar respiration measurements pooled across seasons. Q_{10} values estimated in this manner were less than 2 in all cases, with values of 1.75 for Douglas-fir, 1.59 for western hemlock, and 1.77 for western red cedar.

Diurnal Patterns. The diurnal course of A , g_s , and Ψ_1 was measured on five dominant Douglas-fir trees during the summer of 1999 (Figure 2). These measurements were made using current-year needles within the top 10% of the crown height on 3 clear days: 15 July, 17 August, and 13 September. From mid-July through mid-August, soil moisture availability steadily decreased (Unsworth and others 2004). Air-temperature and vapor-pressure deficit (VPD) values just above the canopy were higher on the August and September measurement days than during the July measurement day. Air temperatures just above the canopy ranged from 15°C in the morning to 28°C , or higher, in the afternoon during August and September, but were typically 5°C cooler throughout the day in July. During the measurement day in July, VPD never exceeded 1.5 kPa, whereas values of more than 3 kPa occurred later in the summer.

Maximum Douglas-fir photosynthesis rates during the sample days in July and August were about $12.5 \text{ mol m}^{-2} \text{ s}^{-1}$ (Figure 2). The values obtained in July and August are similar to other measurements for this species, which are generally made with seedlings and younger trees [see Bond and others (1999) and McDowell and others in press, but see also Thomas and Winner (2002)]. During the September sample day, maximum photosynthetic rates were about 35% lower than in the previous months. Low September photosynthesis rates are likely caused by the accumulating effects of low soil water availability, lower morning humidity, or both. Net photosynthesis declined through the day on all three sampling dates.

Stomatal conductance ranged from 0.5 to $2.5 \text{ mmol m}^{-2} \text{ s}^{-1}$ (Figure 2). As with photosynthesis, stomatal conductance was generally higher during the July sample day than for sample days in August and September. The diurnal pattern of stomatal conductance declined throughout each of the sample days, which roughly parallels changes in photosynthesis.

Leaf Water Potential. Leaf water potential (Ψ_1), averaged over the entire sample day, was consistently more negative for Douglas-fir than for western hemlock and western red cedar (Table 1). All

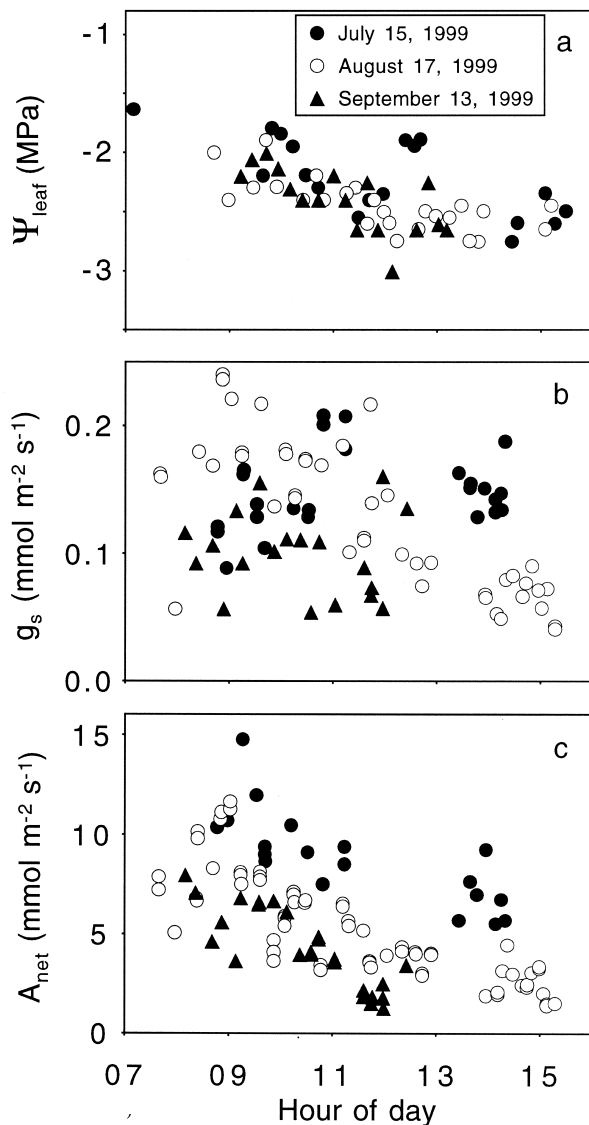


Figure 2. Diurnal values for branch water potential (a), stomatal conductance (b), and net photosynthesis (c) for a 450-year-old Douglas-fir taken on 3 sampling days.

species showed less negative Ψ_1 during winter months compared to summer months, and the December gradient of Ψ_1 in each species nearly matched the hydrostatic gradient of 0.01 MPa m^{-1} . Thus, complete rehydration may occur after the summer drought.

Diurnal Ψ_1 was measured concurrent with gas-exchange measurements for Douglas-fir (Figure 2). The diurnal decline in both A and g_s corresponded to the decline in Ψ_1 ; however, seasonal changes in gas exchange were not related to Ψ_1 . Midday Ψ_1 remained constant throughout the summer, despite the significant decline in soil moisture (Un-

worth and others 2004). Ψ_1 typically reached midday minimum values ranging from -2.5 to -2.6 MPa . Woody species commonly have a species-specific minimum water potential (Hinckley and others 1978), so the observation for Douglas-fir is not unique. Most investigations have reported midday minimum Ψ_1 values that are 0.2 – 0.4 MPa higher than we measured on the old-growth Douglas-fir at Wind River (Running 1976; Bond and Kavanagh 1999; McDowell and others in press). The midday minimum Ψ_1 could help maintain the water-potential gradient required to pull water from roots to leaves in these trees, some of which are nearly 65 m tall (McDowell and others in press). The gravitational potential is -0.65 MPa for these tall trees, and hydraulic resistance of stems is likely to increase with tree size (Ryan and Yoder 1997).

Vapor-pressure Deficit. Net photosynthesis is inversely associated with VPD (Figure 3) and is best described by an exponential decay equation:

$$A = a + b * e^{(-c * \text{VPD})} \quad (1)$$

The equation explains about 66%, 35%, and 64% of the variation in net photosynthesis for July, August, and September measurements, respectively. The regression lines are similar for August and September. During July, however, photosynthesis was about 20% higher at any VPD than for the later months.

Water-use Efficiency

Stable Carbon Isotopes Show Stomatal Limitation of Carbon Use. The instantaneous gas-exchange data for 3 summer days show Douglas-fir needles both close stomata and reduce photosynthesis over the course of a day and as the summer progresses. Such instantaneous measurements are useful to understand the dynamic behavior of both g_s and A . However, the integration period of these measurements is on the order of seconds to minutes.

Douglas-fir, western hemlock, and western red cedar have different c_i/c_a ratios, suggesting that the WUE differed among these tree species (Table 2). Specifically, western hemlock had the highest c_i/c_a , Douglas-fir was intermediate, and western red cedar had the lowest c_i/c_a . Both short-term gas-exchange observations and the long-term carbon isotope analyses indicate the same relative rankings. The c_i/c_a ratios did not remain constant throughout the canopy (Figure 4). Instead, c_i/c_a ratios increased with depth into the canopy, which is a pattern seen in many forest ecosystems (Ehleringer and others 1993).

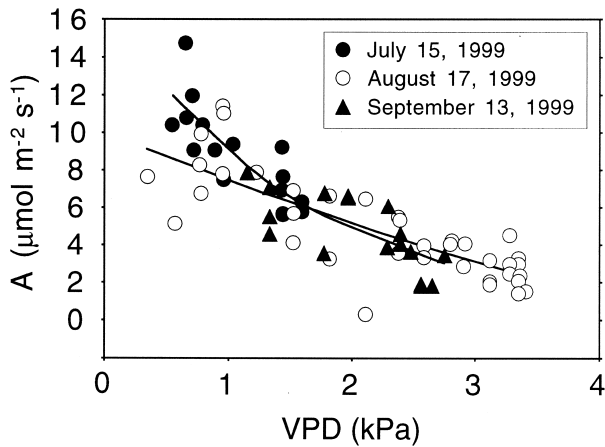


Figure 3. The response of photosynthesis (A) to vapor-pressure deficit (VPD) for a 450-year-old Douglas-fir. Samples were collected on 3 days representing early, middle, and late drought (July, August, and September, respectively).

Using equations from Farquhar and colleagues (1989) and atmospheric observations (Figure 4), the carbon isotope data were converted to expected long-term c_i values (Table 2). Although differences in the c_i values were less than 33 ppm within canopy trees, the differences in c_i between canopy trees and understory vegetation approached 110 ppm. Large differences in c_i between species suggest biological controls over gas exchange range widely with height and across species within this forest.

The most likely scenario is that decreases in photosynthesis and stomatal conductance observed for foliage at the top of Douglas-fir during the day, and the growing season, are typical, and that stomatal closure functionally limits carbon gain for much of the life of these needles. Isotopic analysis suggests that needles in upper portions of the canopy are the ones for which gas exchange is most limited by stomatal constraints (Table 2). Photosynthesis by leaves of vegetation in the understory is least constrained by stomata, while stomata on those needles in the middle of the canopy imposed an intermediate constraint. These isotope ratios and c_i profiles with canopy height are similar to values reported in another old-growth forest in the Pacific Northwest (Buchmann and others 1998b), but are larger than differences observed in developing coniferous canopies (Zhang and others 1993; Marshall and Zhang 1994). Carbon isotope data not shown indicate that needles and small stems falling to the ground originate mainly from the upper canopy.

Trends in Water Use with Canopy Height. Foliage was collected along complete height profiles of two species—Douglas-fir and western hemlock—adjacent to the location of hemispheric photograph measurements. The $\delta^{13}\text{C}$ value of foliage indicates that WUE increased with increasing canopy height for Douglas-fir (Figure 4) but not for western hemlock (data not presented). WUE was a plastic characteristic for Douglas-fir and increased with increasing light availability, but was unable to change for western hemlock.

Isotopic trends with change in elevation in the canopy result from changes in the physiology of the foliage, as well as changes in atmospheric CO_2 concentration in the canopy. The variations in $\delta^{13}\text{C}_p$ that occur with change in depth into the canopy (Figure 4) probably reflect isotopic change caused by increasing c_a that occurs with decreasing canopy height (Medina and Minchin 1980), yet the changes in $\delta^{13}\text{C}_p$ were much larger than the observed decreases in $\delta^{13}\text{C}_a$. Therefore, the paired $\delta^{13}\text{C}_p$ and $\delta^{13}\text{C}_a$ data suggested that relatively large changes in carbon isotope discrimination occurs throughout the canopy profile; that is, the response of photosynthesis by vegetative components within the canopy changed so that stomatal constraints decreased with decreasing light levels. In this respect, the long-term isotope ratio data are consistent with short-term observations of gas exchange (Thomas and Winner 2002, Table 1). However, leaf N concentration also declined significantly with tree height for Douglas-fir but not for western hemlock (T.M.H. unpublished data). Leaf N exerts a strong control over A (Field and Mooney 1986). Therefore, the differences in the vertical profiles of $\delta^{13}\text{C}_p$ may also reflect changes in photosynthetic capacity for Douglas-fir but not for western hemlock.

The aggregated impact of changes in the c_i/c_a ratio with different species and with different height effects can be assessed using a Keeling-plot approach (Buchmann and others 1997) (Figure 5). By sampling the carbon isotope ratio of atmospheric CO_2 ($\delta^{13}\text{C}_a$) within the canopy and relating this with the absolute CO_2 concentration measured at the same time, it is possible to obtain an integrated estimate of the carbon isotope ratio of CO_2 respired by all elements of the ecosystem ($\delta^{13}\text{C}_R$). Air repeatedly sampled within the Wind River canopy crane primary forest has a $\delta^{13}\text{C}$ value of -26.1‰ . If the $\delta^{13}\text{C}_R$ value is approximately the same as the $\delta^{13}\text{C}_p$ value, there is no isotopic fractionation during respiration (Lin and Ehleringer 1997). However, at the Wind River site, the $\delta^{13}\text{C}_R$ is not similar to long-term $\delta^{13}\text{C}_p$ values of the

Table 2. Carbon Isotope Ratios, Isotope Discrimination, and c_i/c_a Ratios

Species	Height(m)	$\delta^{13}C_p$ (‰)	$\delta^{13}C_a$ (‰)	Observed c_i/c_a	Predicted c_i/c_a	Observed Δ (‰)	Predicted Δ (‰)
Douglas-fir	53	-27.0	-8.6	0.51	0.62	16.0	18.4
Western hemlock	53	-27.8	-8.6	0.52	0.65	16.2	19.2
Western red cedar	53	-25.8	-8.6	0.41	0.56	13.6	17.1
Douglas-fir	24	-27.9	-8.5	0.61	0.67	18.1	19.5
Western hemlock	24	-29.5	-8.5	0.69	0.73	20.0	21.0
Western red cedar	24	-27.5	-8.5	0.61	0.65	18.2	19.0
Pacific silver fir	1.5	-33.8	-10.0	—	0.86	—	23.8
Vine maple	1.5	-31.3	-10.0	—	0.75	—	21.3
Oregon grape	0.3	-32.2	-10.8	—	0.75	—	21.4
Feather moss	0	-32.3	-10.8	—	0.76	—	21.5

A comparison of the carbon isotope ratios of plant materials and atmospheric CO_2 , ratios of intercellular to ambient CO_2 levels (c_i/c_a), and carbon isotope discrimination by dominant tree species and common understory species at the Wind River canopy crane site. Isotopic ratio data are means of nine samples for canopy trees and four samples for understory species. The predicted and c_i/c_a ratios are based on $\delta^{13}C_a$ and $\delta^{13}C_p$ observations, whereas observed and c_i/c_a values are based on gas-exchange measurements (W.E.W. and S.C.T. personal communication).

two most common tree species, suggesting that some factor is causing these two parameters to deviate from each other. Calculations of ecosystem-level $\delta^{13}C_R$ values also reveal a discrepancy, suggesting that late-season canopy-level gas-exchange behavior is different from earlier parts of the growing season. The sum of the $\delta^{13}C_R$ and the $\delta^{13}C_a$ value of tropospheric CO_2 (-7.8‰) is the integrated discrimination (Δ_e) value for the entire ecosystem (Buchmann and others 1998a). Summing the $\delta^{13}C$ values for respiration and ambient CO_2 results in a Δ_e value of 18.3‰. Although this Δ_e value is similar to that of the upper-canopy needles of *Pseudotsuga menziesii*, which is the dominant component of this ecosystem, the Δ_e value is different from that of the other two dominant species. In addition, the Δ_e value is also different from midcanopy Δ_e values for all three dominant tree species, which must be included in an integrated analysis (Table 2). When the Δ_e value is weighted for different species and leaf-area distributions, the predicted Δ_e is greater than the observed 18.3‰.

Late-season Water Stress. The leaf-level c_i/c_a values reflect the degree of stomatal control over photosynthesis that are over and above any temperature-induced or light-induced limitations. The c_i/c_a ratios of canopy components late in the season were lower than expected based on integrated-season isotope ratio measurements (Figure 6). Although there is an expected significant correlation between the two independent estimates of c_i/c_a behavior ($r = 0.95$), the slope of this relationship is significantly less than unity. The deviations between long-term and short-term c_i/c_a values are

greater for needles in the upper portions of the canopy than in midportions of the canopy for all three dominant tree species. Thus gas exchange at the canopy level, in later stages of the growing season, is likely more constrained by stomatal activity than in earlier growth periods. Upper-canopy needles were impacted more than mid-canopy needles for all three species. Such increased stomatal constraint with season and with canopy position would be over and above any downregulation acclimation responses that occurred.

Biogenic Hydrocarbon Emissions and Terrestrial Carbon Exchange

Measured Terpene Emissions. Fourteen monoterpenes were positively identified from trees at the Wind River site (Table 3). The composition of monoterpenes emitted differs among plant species, season, and needle age (Arey and others 1991; Lerdau and others 1995; Constable and others 1999). For May 1997, the predominant monoterpene emitted by Douglas-fir and western hemlock is α -pinene. However, for western red cedar and Pacific silver fir, the dominant monoterpenes are thujone and Δ^3 -carene, respectively. During the summer of 1997, additional analysis resulted in expanding the list of BHCs to include α -pinene, β -pinene, Δ^3 -carene, limonene, camphene, and myrcene. On average, α -pinene was 51% of the total monoterpene emissions for Douglas-fir and 38% of the total emissions for western hemlock. The second highest monoterpene was β -pinene, averaging 26% of the total for Douglas-fir and 22%

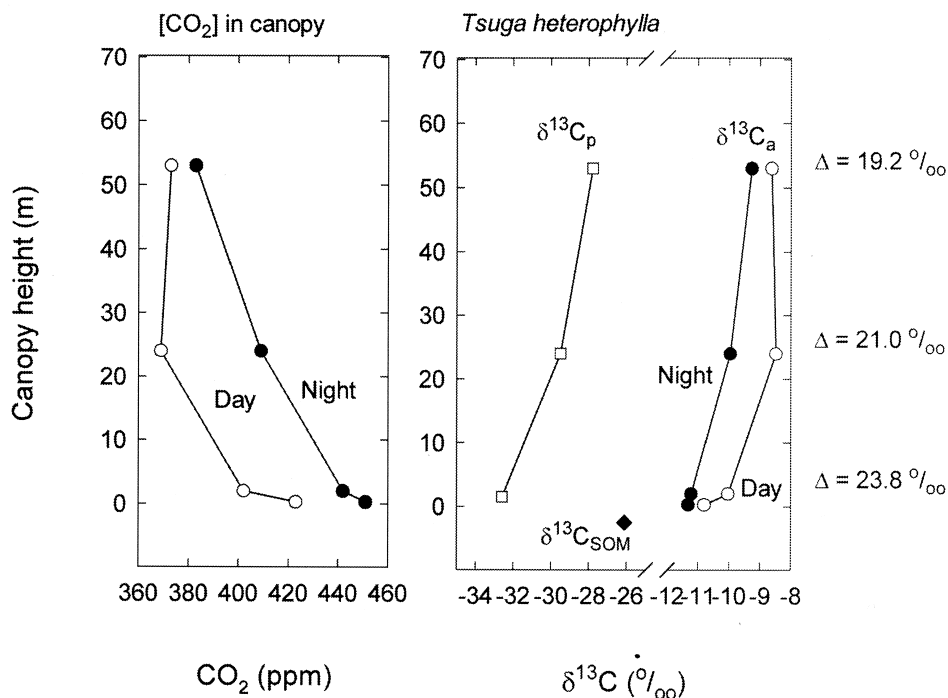


Figure 4. Variations in $[CO_2]$ and carbon isotope ratios of canopy CO_2 ($^{13}C_a$), plant organic matter ($^{13}C_p$), and soil organic matter ($^{13}C_{SOM}$) at the Wind River canopy crane forest site. Symbols represent averages for $\delta^{13}C_a$ ($n = 2$), $\delta^{13}C_p$ ($n = 9$), and $\delta^{13}C_{SOM}$ ($n = 5$). Needle samples were collected at the canopy top and midcanopy from sun-exposed south-facing branches of Douglas-fir. Each symbol in Figures 4 and 6 represents the average of the three trees sampled per species; the error within the measurements was smaller than the symbol; ppm, parts per million.

of the total for western hemlock. In all samples, α -pinene, β -pinene, and limonene together comprised more than 64% of the emissions from all trees.

Douglas-fir and western hemlock branches from the Wind River site were used to measure BHC emission rates. The total monoterpene emission rates for Douglas-fir ranged from $0.009 \mu g C g^{-1} h^{-1}$ when ambient temperatures were near $14^\circ C$ to a maximum of $4.5 \mu g C g^{-1} h^{-1}$ measured at $40^\circ C$. The total monoterpene emission rates for western hemlock ranged from $0.07 \mu g C g^{-1} h^{-1}$ at $15^\circ C$ to $6.3 \mu g C g^{-1} h^{-1}$ measured at $42^\circ C$ (Pressley and others in press).

Branch enclosure data were used to determine standard emission rates (Es) and the corresponding temperature coefficient (Figure 7). The large scatter in the data reflects natural variability and measurement error. The measured values for the temperature-dependent monoterpene emissions for Douglas-fir are $0.15 K^{-1}$ with a standard emission rate of $0.3 \mu g C g^{-1} h^{-1}$. These parameters can be used to estimate accumulated loss of carbon due to terpene emissions during 1998 and 1999.

Biogenic Hydrocarbon and Net Carbon Exchange. To place BHC emissions in the context of the net carbon exchange of the whole forest, estimates of net fluxes of C and BHC are needed. Net C balance was determined using eddy-flux techniques (Wofsy and others 1993; Hollinger and others 1994; Black and others 1996; Valentini and others 1996; Greco and Baldocchi 1996). Terpene emissions for the forest were estimated from the Guenther emission algorithm and the site-specific emission factors from Pressley (1999) incorporated into a dynamic forest canopy model for each 30-min period of the growing season.

The net carbon exchange, the terpene flux, and the resulting percentage of terpene to CO_2 changed throughout 1998 (Figure 8). For the period from midsummer through late winter, the accumulated net carbon exchange increased to a maximum of $+7 mol C m^{-2}$ (positive indicates net flow to the atmosphere) and then decreased. Terpene fluxes averaged approximately 1% of the net carbon loss during 1998 and also during the net carbon uptake in 1999 (data not presented). The uncertainty in the predicted terpene emissions is estimated at approximately a factor of 2 so that the estimated

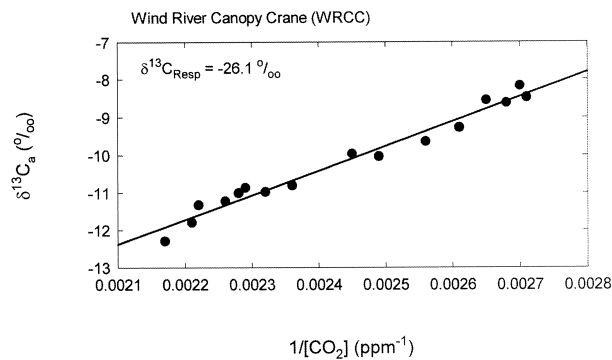


Figure 5. A Keeling plot showing the carbon isotope ratios of canopy CO_2 ($^{13}\text{C}_a$) and the CO_2 concentration within the canopy. The intercept reflects $\delta^{13}\text{C}_R$, the integrated $\delta^{13}\text{C}$ ratio of CO_2 respired from the ecosystem; ppm, parts per million.

percentage of terpene to CO_2 ranges between 0.5% and 2%. At times when the net carbon exchange approached zero, the fraction of terpenes increased rapidly. Therefore, carbon loss by volatile emissions is a measurable portion of the net carbon exchange, and when net carbon exchange is near zero, terpene emissions can be an important component of the carbon budget.

Scaling from Trees to Stands: Predictions of Whole-ecosystem Latent Energy Flux and Gross Primary Production

We applied available meteorologic data from the site to model the latent energy (LE) flux and gross primary production (GPP) fluxes for 1998 and 1999 (Figure 9). Meteorologic data were available for 86% of days in 1998 and for 66% of the days in 1999. Modeled estimates of LE and GPP for days 51–360 in 1998 were $1248 \text{ MJ m}^{-2} \text{ y}^{-1}$ and $2303 \text{ g C m}^{-2} \text{ y}^{-1}$, respectively, and for days 1–236 in 1999 were $1144 \text{ MJ m}^{-2} \text{ y}^{-1}$ and $1869 \text{ g C m}^{-2} \text{ y}^{-1}$. LE flux is the sum of canopy transpiration and evaporation from the soil surface and wetted leaf surfaces. The predictions show that, for the first 2 months of the year, cloudy conditions and cool temperatures kept LE flux at low levels. As insolation and temperatures increased in March, both water fluxes to the atmosphere and production rose toward their peak values. The key controls on LE demand, VPD and GPP (insolation) are tightly correlated, so cycles of cloudy, humid days and bright, dry days control patterns of evapotranspiration and carbon assimilation until midsummer. However, once soil moisture begins to decline after day 200, water supply becomes limiting, stomatal

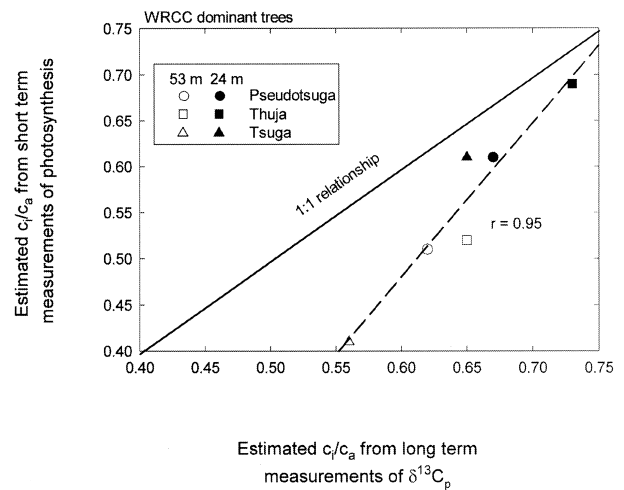


Figure 6. The correlation between the observed and predicted c_i/c_a ratios of needles from Douglas-fir, western hemlock, and western red cedar. The short-term c_i/c_a ratio is determined from in situ photosynthesis gas-exchange measurements (Thomas and Winner 2002, and unpublished data), and the long-term estimate is based on $\delta^{13}\text{C}_p$ measurements in Table 1. WRCC, Wind River canopy crane. Each symbol in Figures 4 and 6 represents the average of the three trees sampled per species; the error within the measurements was smaller than the symbol.

opening is constricted, and both LE flux and GPP are reduced. The estimates of GPP are similar to those of Harmon and colleagues (2004), but much higher than those of Paw U and coworkers (2004).

DISCUSSION

Predictive models of complex forest ecosystems must make assumptions and simplifications, as is the case for the physiological process modeling approach we demonstrate here. Our purpose for modeling is not only to better understand carbon use in the study forest, but also to guide thinking to improve the quality of the model and increase the use of model parameters derived from on-site measurements. In the present report, we present simulation results that are based in part on stand-specific parameter estimates, but also incorporate many “generic” assumptions and parameters derived from other forest communities (Williams and others 1996). Many of the empirical results presented are consistent with our modeling assumptions. For example, the SPA model assumes that stomatal conductance maintains leaf water potential above a critical threshold level, and this assumption is broadly supported by the diurnal and seasonal patterns of gas exchange reported here for

Table 3. Monoterpene-emission Composition of Dominant Species

Compound	Douglas-fir	Western Red Cedar	Pacific Silver Fir	Western Hemlock
α -Pinene	D	T	D	D
β -Pinene	D	T	D	D
Limonene	D	D	D	D
Δ^3 -Carene	D	D	D	T
Sabinene	T	T	T	T
Camphene	T		T	T
Myrcene	T	T	T	T
2-Carene	T	T	T	T
α -Phellandrene	T		T	T
Tricyclene	T		T	T
β -Phellandrene				T
Thujene	T			
α -Terpinolene	T	T	T	T
Thujone		D		

Monoterpene-emission composition for four dominant species at the Wind River Canopy Crane Research Facility. Dominant (D) compounds are those with concentrations greater than 10% of the total versus trace (T) concentrations.

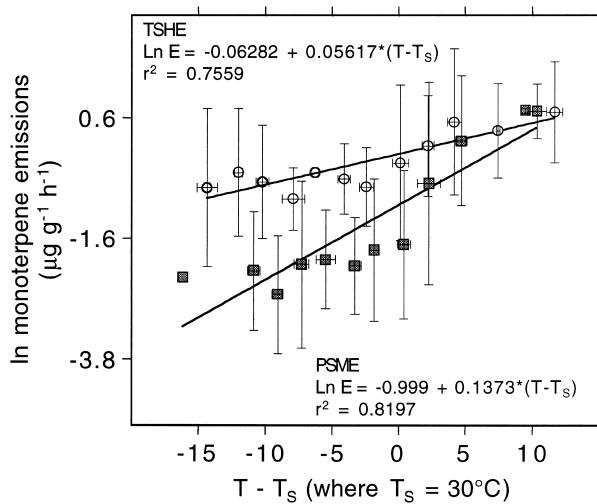


Figure 7. Monoterpene emissions ($\ln E$) plotted against temperature deviation from standard temperature where data are block-averaged by 2°C temperature intervals. Error bars indicate standard deviation from the mean.

Douglas-fir. Strong diurnal declines in stomatal conductance and photosynthesis that are more pronounced during late-season drought conditions are likewise consistent with model assumptions. However, the SPA model incorporates neither interspecific differences in gas-exchange parameters nor seasonal changes in photosynthetic physiology, and our results indicate that both of these sources of variation are large (Table 1). In addition, use of the most recent estimates for LAI and vertical distribution (Thomas and Winner 2000; Parker and others 2004), would be preferable to assuming a

uniform, vertical distribution of foliage through the canopy.

Measurements of parameters that are not yet assessed are needed to better simulate processes linking physiology to forest growth and structure. For example, measurements of carbon allocation would be needed before we could reach a strong conclusion about the timing and location of carbon sinks and sources within this forest. Improved estimates of photosynthetic parameters [such as the maximum velocity of RuBP carboxylation (V_{cmax}) and light-saturated potential rate of electron transport (J_{max})] for all species at multiple canopy heights are also needed to test the assumption of a single vertical gradient through the canopy. In addition, we have only limited information on the rooting depth and source of water acquisition in this forest, and such data are also needed for model parameterization. Much of the physiological process work at the Wind River site has emphasized measurements on canopy foliage. However, understanding the timing, size, and controls over net ecosystem exchange also requires tissue-level measurements of carbon fluxes from soil, stems, and downed wood. Currently only limited data are available on these components at the site (J. Klopatsek unpublished data). Such measurement would make possible independent estimates of ecosystem respiration and net primary production.

The large species-specific differences in physiology shown here provide a compelling argument as to why a modeling approach founded on both physiological and ecological processes is ultimately necessary to understanding and predicting forest

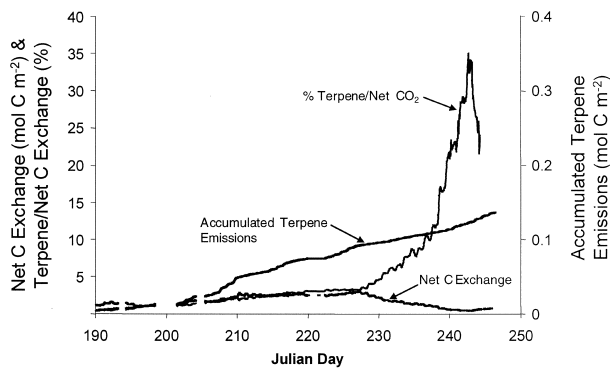


Figure 8. Wind River canopy crane eddy-flux data. Accumulated net carbon (C) exchange (as CO₂) measured with eddy-correlation methods at the Wind River canopy crane site and the estimated accumulated terpene emissions during 1998.

carbon flux. The dominant species at the Wind River canopy crane site differ substantially in physiological parameters central to understanding carbon flux. The observed photosynthetic differences are consistent with long-standing generalizations [compare Bazzaz (1979) and Teskey and Shestha (1985)], in that Douglas-fir showed a higher light-saturated photosynthetic rate, dark respiration rate, and light-saturation point than did the later successional western hemlock and western red cedar. Douglas-fir also showed a relatively low emission rate for terpenes, consistent with recent comparisons across trees and forests of different successional status (Martin and Guenther 1995; Klinger and others 1998). However, contrary to some previous generalizations, the early-successional but long-lived Douglas-fir showed a conservative water-use strategy compared to the later successional species [compare Bazzaz (1979)]. Our results thus indicate that, as western hemlock gradually replaces Douglas-fir in this stand, not only will there be substantial changes in the amount and vertical distribution of leaf area in the canopy (Thomas and Winner 2000), gas-exchange characteristics of canopy foliage will also change dramatically. For example, while terpene fluxes account for approximately 1% of net carbon loss from the forest at present, this value is likely to increase substantially as the stand becomes increasingly dominated by western hemlock.

Based on the physiological process model presented here, we estimate current GPP (assuming an LAI of 9.6) at 24.6 Mg C ha⁻¹ y⁻¹. Revision of this estimate to take into account a recent measurement of LAI of 8.6 (Thomas and Winner 2000) gives a GPP of about 22 Mg C ha⁻¹ y⁻¹, a value that

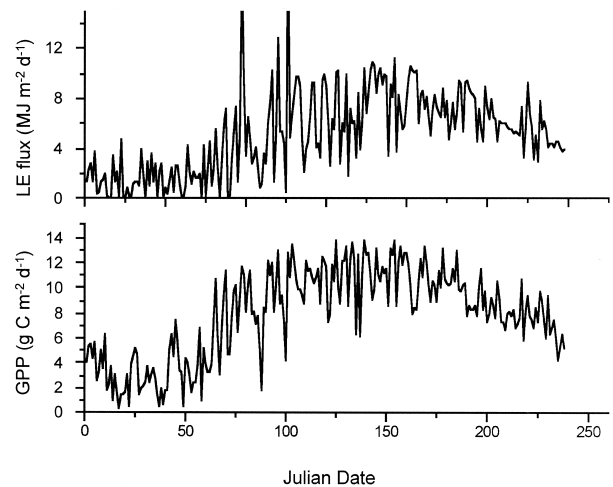


Figure 9. Simulated total canopy latent energy (LE) flux and gross primary productivity (GPP) in 1999 for the old-growth Wind River forest in 1999, based on locally parameterized soil-plant-atmosphere model.

is similar to that presented by Harmon and colleagues (2004). Using eddy-flux methods, Paw U and coworkers (2004) estimate a net carbon uptake of 2.1 Mg C ha⁻¹ y⁻¹ and a net respiration (at 3-m height) of 9.2 Mg C ha⁻¹ y⁻¹, yielding a “gross” productivity above 3 m in height of 11.3 Mg C ha⁻¹ y⁻¹. However, this gross productivity figure necessarily excludes respiration components above 3 m (that is, foliar respiration, sapwood respiration, and heart rot). Harmon and colleagues (2004) estimate these components at about 6.5 Mg C ha⁻¹ y⁻¹. In sum, all three estimates of GPP fall within about 4 Mg C ha⁻¹ y⁻¹. The three approaches for analysis of carbon flux thus provide initial results that are similar and will likely converge as more site-specific information is gathered and as models improve. The acquisition of information on physiological and ecological processes will continue to play an essential role in explaining forest ecosystem processes, in refining estimates of carbon balance derived from biomass inventory analysis and eddy-covariance measurements, and in resolving difference in carbon-flux rates determined by different measurement techniques.

ACKNOWLEDGEMENTS

This research was supported by the Office of Science, Biological and Environmental Research Program (BER), US Department of Energy (DOE), through the Western Regional Center (WESTGEC) of the National Institute for Global Environmental

Change (NIGEC) under Cooperative Agreement DE-FC03-90ER61010. Authors who are investigators with WESTGEC funds to work at the site include W. E. Winner, J. Berry, B. J. Bond, T. Hinckley, J. Ehleringer, B. Lamb, and S. C. Thomas. Dr. Thomas Suchanek, WESTGEC Director, along with Dr. Susan Ustin and the WESTGEC staff, have helped create the focused interest in analysis of carbon balance at this site. We also greatly appreciate the efforts of Dr. David Shaw, Director of the Wind River canopy crane site, who has provided assistance in organizing research and providing logistical support at the site. We are particularly indebted to Mr. Mark Creighton, and those who "bell" the crane, for safely moving us through the forest canopy with the precision and care necessary to gather physiological data in the forest canopy without damaging trees.

REFERENCES

- Aber JD, Federer C. 1992. A generalized, lumped-parameter model of photosynthesis, evaporation and net primary production in temperate and boreal forest ecosystems. *Oecologia (Berl)* 92:463–74.
- Aber JD, Reich PB, Goulden ML. 1996. Extrapolating leaf CO₂ exchange to the canopy: a generalized model of forest photosynthesis compared with measurements by eddy correlation. *Oecologia (Berl)* 106:257–65.
- Arey J, Winer AM, Atkinson R, Aschmann SM, Long WD, Morrison CL, Olszyk DM. 1991. Terpenes emitted from agricultural species found in California's central valley. *J Geophys Res* 96:9329–36.
- Bazzaz FA. 1979. The physiological ecology of plant succession. *Annu Rev Ecol Syst* 10:351–71.
- Black TA, Den Hartog G, Neumann HH, Blanken PD, Yang PC, Russell C, Nescic Z, Lee X, Chen SG, Staebler R, Novak MD. 1996. Annual cycles of water vapour and carbon dioxide fluxes in and above a boreal aspen forest. *Global Change Biol* 2:219–29.
- Bond BJ, Farnsworth BT, Coulombe RA, Winner WE. 1999. Foliage physiology and biochemistry in response to light gradients in conifers with varying shade tolerance. *Oecologia (Berl)* 120:183–92.
- Bond BJ, Kavanagh KL. 1999. Stomatal behavior of four woody species in relation to leaf-specific hydraulic conductance and threshold water potential. *Tree Physiol* 19:503–10.
- Buchmann N, Brooks JR, Flanagan LB, Ehleringer JR. 1998a. Carbon isotope discrimination of terrestrial ecosystems. In: Griffiths H, editor. *Stable isotopes: integration of biological, ecological, and geochemical processes*. Oxford: BIOS Scientific. p 203–21.
- Buchmann N, Hinckley TM, Ehleringer JR. 1998b. Carbon isotope dynamics in *Abies amabilis* stands in the Cascades. *Can J For Res* 28:808–19.
- Buchmann N, Kao W, Ehleringer JR. 1997. Influence of stand structure on carbon-13 of vegetation, soils, and canopy air within deciduous and evergreen forests of Utah, United States. *Oecologia (Berl)* 110:109–19.
- Chen JQ, Falk M, Euskirchen E, Paw U KT, Suchanek TH, Ustin SL, Bond BJ, Broszofski KD, Phillips N, Bi RC. 2002. Biophysical controls of carbon flows in three successional Douglas-fir stands based on eddy-covariance measurements. *Tree Physiol* 22:169–77.
- Constable JVH, Litvak ME, Greenberg JP, Monson RK. 1999. Monoterpene emission from coniferous trees in response to elevated CO₂ concentration and climate warming. *Global Change Biol* 5:255–67.
- Croteau R. 1987. Biosynthesis and catabolism of monoterpenoids. *Chem Rev* 87:929–54.
- In: Ehleringer JR, Hall A, Farquhar GD editors. 1993. *Stable isotopes and plant carbon/water relations*. San Diego: Academic.
- Farquhar GD, Ehleringer JR, Hubick KT. 1989. Carbon isotope discrimination and photosynthesis. *Annu Rev Plant Physiol Mol Biol* 40:503–37.
- Farquhar GD, Von Caemmerer S. 1982. Modelling of photosynthetic response to the environment. *Encycl Plant Physiol [B]* 12:549–87.
- Fehsenfeld F, Calvert J, Fall R, Goldan P, Guenther A, Hewitt CN, Lamb B, Liu S, Trainer M, Westberg H, Zimmerman P. 1992. Emissions of volatile organic compounds from vegetation and the implications for atmospheric chemistry. *Global Biogeochem Cycles* 6:389–430.
- Fessenden JE, Ehleringer JR. 2002. Age-related variations in delta C-13 of ecosystem respiration across a coniferous forest chronosequence in the Pacific Northwest. *Tree Physiol* 22:159–67.
- Flanagan LB, Brooks JR, Varney GT, Berry SC, Ehleringer JR. 1996. Carbon isotope discrimination during photosynthesis and the isotope ratio of respired CO₂ in boreal ecosystems. *Global Biogeochem Cycles* 10:629–40.
- Greco S, Baldocchi DD. 1996. Seasonal variations of CO₂ and water vapour exchange rates over a temperate deciduous forest. *Global Change Biol* 2:183–97.
- Guenther A, Geron C, Pierce T, Lamb B, Harley P, Fall R. 1999. Natural emissions of non-methane volatile organic compounds, carbon monoxide, and oxides of nitrogen from North America. *Atmos Environ*.
- Guenther A, Hewitt CN, Erickson D, Fall R, Geron C, Graedel T, Harley P, Klinger L, Lerdau M, McKay WA, others. 1995. A global model of natural volatile organic compound emissions. *J Geophys Res* 14:183–97.
- Guenther A, Zimmerman P, Harley P, Monson R, Fall R. 1993. Isoprene and monoterpene emission rate variability: model evaluations and sensitivity analyses. *J Geophys Res* 12:609–12.
- Harmon ME, Bible K, Ryan MG, Shaw DC, Chen H, Klopatek J, Li X. 2004. Production, respiration, and overall carbon balance in an old-growth *Pseudotsuga-Tsuga* forest ecosystem. *Ecosystems* 7:498–512.
- Hinckley TM, Lassoie JP, Running SW. 1978. Temporal and spatial variations in the water status of forest trees. *For Sci Monogr* 20:1–72.
- Hollinger DY, Kelliher FM, Byers JN, Hunt JE, McSeveny TM, Weir PL. 1994. Carbon dioxide exchange between an undisturbed old-growth temperate forest and the atmosphere. *Ecology* 75:134–50.

- Hunt JE, McSeveny TM, Weir PL. 1994. Carbon dioxide exchange between an undisturbed old-growth temperate forest and the atmosphere. *Ecology* 75:134–50.
- Jacob DJ, Wofsy SC. 1988. Photochemistry of biogenic emissions over the Amazon forest. *J Geophys Res* 93:1477–86.
- Jarvis PG. 1993. Prospects for bottom-up models. In: Ehleringer JR, Field CB editors. *Scaling physiological processes: leaf to globe* San Diego: Academic.
- Juuti S, Arey J, Atkinson R. 1990. Monoterpene emission rate measurements from a Monterey pine. *J Geophys Res* 95:7515–9.
- Klinger LF, Greenberg J, Guenther A, Tyndall G, Zimmerman P, M'Bangi M, Moutsambotá J-M, Kenfack D. 1998. Patterns in volatile organic compound emissions along a savanna-rainforest gradient in central Africa. *J Geophys Res* 103:1443–54.
- Law B, Williams M, Anthoni PM, Baldocchi DD, Unsworth MH. 2000. Measuring and modeling seasonal variation of carbon dioxide and water vapor exchange of a *Pinus ponderosa* forest subject to soil water deficit. *Global Change Biol* 6:613–30.
- Lerdau M, Matson P, Fall R, Monson R. 1995. Ecological controls over monoterpene emissions from Douglas-fir (*Pseudotsuga Menziesii*). *Ecology* 76:2640–7.
- Lewis JD, McKane RB, Tingey DT, Beedlow PA. 2000. Vertical gradients in photosynthetic light response within an old-growth Douglas-fir and western hemlock canopy. *Tree Physiol* 20:447–56.
- Lin G, Ehleringer JR. 1997. Carbon isotopic fractionation does not occur during dark respiration in C₃ and C₄ plants. *Plant Physiol* 114:391–4.
- Litvak M. 1997. Environmental and biotic controls over the production and emission of nonmethane hydrocarbons from trees [PhD thesis]. Boulder: University of Colorado.
- Marshall JD, Zhang J. 1994. Carbon isotope discrimination and water-use efficiency in native plants of the north-central Rockies. *Ecology* 75:1887–95.
- Martin PH, Guenther AB. 1995. Insights into the dynamics of forest succession and non-methane hydrocarbon trace gas emissions. *J Biogeogr* 22:493–9.
- McDowell NG, Phillips N, Lunch C, Bond BJ, Ryan MG. 2002. An investigation of hydraulic limitation and compensation in large, old Douglas-fir trees. *Tree Physiol* 22:763–74.
- Medina E, Minchin P. 1980. Stratification of $\delta^{13}\text{C}$ values of leaves in Amazonian rainforests. *Oecologia (Berl)* 45:355–78.
- Ögren E, Evans JR. 1993. Photosynthetic light-response curves. I. The influence of CO₂ partial pressure and leaf inversion. *Planta (Berl)* 189:182–90.
- Parker GG, Harmon ME, Lefsky MA, Chen J, Van Pelt R, Weiss SB, Thomas SC, Winner WE, Shaw DC, Franklin JF. 2004. Three-dimensional structure of an old-growth *Pseudotsuga-Tsuga* canopy and its implications for radiation balance, microclimate, and atmospheric gas exchange. *Ecosystems* 7:440–53.
- Paulson SE, Flagan RC, Seinfeld JH. 1992. Atmospheric photo-oxidation of isoprene. Part I: The reactions of isoprene with hydroxyl radical and ground state atomic oxygen. *Int J Chem Kinet* 24:79–101.
- Paw U KT, Falk M, Suchanek TH, Ustin SL, Chen J, Park Y-S, Winner WE, Thomas SC, Hsiao TC, Shaw RH and others. 2004. Carbon dioxide exchange between an old-growth forest and the atmosphere. *Ecosystems* 7:513–24.
- Phillips N, Bond BJ, McDowell NG, Ryan MG. 2002. Canopy and hydraulic conductance in young, mature and old Douglas-fir trees. *Tree Physiol* 22:205–11.
- Pressley S, Lamb B, Westberg H, Claiborn C. In review. Monoterpene emissions from a Pacific Northwest old growth forest. In: American Geophysical Union Fall Meeting, EOS, Transactions.
- Pressley S, Lamb B, Westberg H, Guenther A. Monoterpene emissions from a Pacific Northwest old growth forest. *Tree Physiol*. In press.
- Rasmussen RA, Khalil MAK. 1988. Isoprene over the Amazon basin. *J Geophys Res* 93:1417–21.
- Running SW. 1976. Environmental control of leaf water conductance in conifers. *Can J For Res* 6:104–12.
- Running SW, Coughlan JC. 1988. A general model of forest ecosystem processes of regional applications. I. Hydrologic balance, canopy gas exchange and primary production processes. *Ecol Modell* 42:125–54.
- Running SW, Gower ST. 1991. A general model of forest ecosystem processes for regional applications. II. Nitrogen budgets and carbon partitioning. *Tree Physiol* 9:147–60.
- Ryan MJ, Yoder BJ. 1997. Hydraulic limits to tree height and tree growth. *Bioscience* 47:235–42.
- Saxton KE, Rawls WJ, Romberger JS, Papendick RI. 1986. Estimating generalized soil-water characteristics from texture. *J Soil Sci Soc Am* 90:1031–6.
- Sharkey TD, Loreto F, Delwiche DF. 1991a. The biochemistry of isoprene emission from leaves during photosynthesis. In: Sharkey TD, Holland EA, Mooney HA editors. *Trace gas emissions from plants* San Diego: Academic.
- Sharkey TD, Loreto F, Delwiche DF. 1991b. High carbon dioxide and sunshade effects on isoprene emissions from oak and aspen tree leaves. *Plant Cell Environ* 14:333–8.
- Talbot RW, Beecher KM, Harriss RC, Cofer WR. 1988. Atmospheric geochemistry of formic and acetic acids at a mid-latitude temperate site. *J Geophys Res* 93:1638–52.
- Thomas SC, Winner WE. 2000. Leaf area index of an old-growth Douglas-fir forest estimated from direct structural measurements in the canopy. *Can J For Res* 30:1922–30.
- Thomas SC, Winner WE. 2002. Photosynthetic differences between saplings and adult trees: an integration of field results via meta-analysis. *Tree Physiol* 22:117–27.
- Unsworth MH, Phillips N, Link T, Bond BJ, Falk M, Harmon ME, Hinckley TM, Marks D, Paw U KT. 2004. Components and controls of water flux in an old-growth Douglas-fir-western hemlock ecosystem. *Ecosystems* 7:468–81.
- Valentini R, De Angelis P, Matteucci G, Monaco R, Dore S, Scarascia Mugnozza GE. 1996. Seasonal net carbon dioxide exchange of a beech forest with the atmosphere. *Global Change Biol* 2:199–207.
- Westberg H, Zimmerman P. 1993. Analytical methods used to identify nonmethane organic compounds in ambient atmospheres. In: Newman L editor. *Measurement challenges in atmospheric chemistry* Washington (DC): American Chemical Society. [Advances in Chemistry Series 232].
- Williams M, Eugster W, Rastetter EB, McFadden JP, Chapin FS. 2000. The controls on net ecosystem productivity along an arctic transect: a model comparison with flux measurements. *Global Change Biol* 6:(Suppl 1)116–26.

- Williams M, Malhi Y, Nobre A, Rastetter EB, Grace J, Pereira MGP. 1998. Seasonal variation in net carbon exchange and evapotranspiration in a Brazilian rain forest: a modelling analysis. *Plant Cell Environ* 21:953–68.
- Williams M, Rastetter EB, Fernandes DN, Goulden ML, Wofsy SC, Shaver GR, Melillo JM, Munger JW, Fan S-M, Nadelhoffer KJ. 1996. Modelling the soil–plant–atmosphere continuum in a *Quercus–Acer* stand at Harvard Forest: the regulation of stomatal conductance by light, nitrogen and soil/plant hydraulic properties. *Plant Cell Environ* 19: 911–27.
- Wofsy SC, Goulden ML, Munger JW, Fan SM, Bakwin PS, Dube BC, Bassow SL, Bazzaz FA. 1993. Net exchange of CO₂ in a mid-latitude forest. *Science* 260:1314–7.
- Zhang JW, Marshall JD, Jaquish BC. 1993. Genetic differentiation in carbon isotope discrimination and gas exchange in *Pseudotsuga menziesii*: a common-garden experiment. *Oecologia (Berl)* 93:80–7.